ELSEVIER

Biophysical Chemistry 76 (1999) 161–183

Biophysical Chemistry

Review

Interactions of α-helices with lipid bilayers: a review of simulation studies

Phil C. Biggin[a], Mark S.P. Sansom[b,*]

[a] *The Salk Institute for Biological Studies, 10010 North Torrey Pines Road, La Jolla, CA 92109, USA*
[b] *Laboratory of Molecular Biophysics, Department of Biochemistry, University of Oxford, South Parks Road, Oxford, OX1 3QU, UK*

Received 8 October 1998; received in revised form 10 December 1998; accepted 11 December 1998

Abstract

Membrane proteins, of which the majority seem to contain one or more α-helix, constitute approx. 30% of most genomes. A complete understanding of the nature of helix/bilayer interactions is necessary for an understanding of the structural principles underlying membrane proteins. This review describes computer simulation studies of helix/bilayer interactions. Key experimental studies of the interactions of α-helices and lipid bilayers are briefly reviewed. Surface associated helices are found in some membrane-bound enzymes (e.g. prostaglandin synthase), and as stages in the mechanisms of antimicrobial peptides and of pore-forming bacterial toxins. Transmembrane α-helices are found in most integral membrane proteins, and also in channels formed by amphipathic peptides or by bacterial toxins. Mean field simulations, in which the lipid bilayer is approximated as a hydrophobic continuum, have been used in studies of membrane-active peptides (e.g. alamethicin, melittin, magainin and dermaseptin) and of simple membrane proteins (e.g. phage Pf1 coat protein). All atom molecular dynamics simulations of fully solvated bilayers with transmembrane helices have been applied to: the constituent helices of bacteriorhodopsin; peptide-16 (a simple model TM helix); and a number of pore-lining helices from ion channels. Surface associated helices (e.g. melittin and dermaseptin) have been simulated, as have α-helical bundles such as bacteriorhodopsin and alamethicin. From comparison of the results from the two classes of simulation, it emerges that a major theoretical challenge is to exploit the results of all atom simulations in order to improve the mean field approach.

* Corresponding author. Tel.: +44 1865 275371; email: mark@biop.ox.ac.uk

0301-4622/99/$ - see front matter
PII: S0301-4622(98)00233-6

1. Introduction

Membrane proteins make up approx. 30% of most genomes [1] and yet high resolution structures are known for only a handful of these proteins. In this context, modelling and simulation studies of membrane proteins and of their interactions with lipid bilayers assume considerable importance. Furthermore, the dynamic interactions of peptides and proteins with membranes have important implications for a wide range of biological problems. From the design of new antimicrobial agents to the translocation of whole proteins across it, an understanding of these processes requires a detailed knowledge of the atomic interactions that govern them.

To provide information on the dynamics of peptide/bilayer interactions at an atomic resolution, and also to perform 'impossible' experiments, an increasingly common approach is to employ molecular dynamics or Monte Carlo simulations (for recent reviews see [2–7]). In molecular dynamics (MD) one simulates the properties of the system according to Newton's laws of motion and consequently this offers time-evolved information, which is frequently (but not necessarily) at the atomistic level. However, the more detailed the simulation system, the more computer power is needed. Thus, in the past, different levels of detail have been employed by different research groups in an attempt to improve the efficiency of sampling of peptide-bilayer interactions. In the review we describe recent simulation studies of the interactions of peptides and proteins with lipid bilayers. As the majority of membrane proteins and membrane-active peptides are α-helical we restrict our attention to simulations of the interactions of α-helices with bilayers. Thus we do not discuss, e.g. the many simulation studies of the small non-α-helical peptide gramicidin A. Simulations of gramicidin are reviewed by Sansom [7] and Roux and Karplus [8].

2. α-Helices and lipid bilayers: some basic principles

Before reviewing simulations per se, its is useful to consider some basic principles of helix/bilayer interactions. A priori there are two orientations of an α-helix with respect to the bilayer which are important (see Fig. 1):

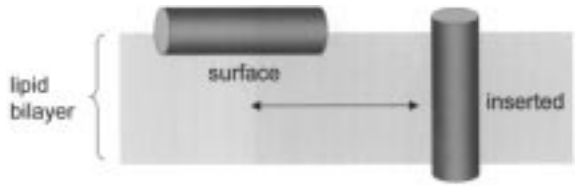

Fig. 1. The 'surface' and 'inserted' orientations of an α-helix relative to a lipid bilayer.

1. parallel to the surface of the bilayer and outside of the hydrophobic core, i.e. a 'surface' orientation; and
2. perpendicular to the bilayer surface, spanning the hydrophobic core of the bilayer, i.e. an 'inserted' orientation.

These two orientations of an α-helix relative to a bilayer have been suggested to be the most favourable on the basis of continuum free energy calculations of the interaction of a 25mer polyalanine helix with a somewhat idealised, purely hydrophobic membrane [9]. Furthermore, the limited number of crystallographic structures of membrane proteins indicate that these two orientations are preferred, with the transmembrane (TM) orientation being found in almost all α-helical integral membrane proteins.

This orientational preference is thought to play an important role in membrane protein assembly, effectively reducing the number of degrees of freedom available to a protein whilst folding within a membrane. This idea is embodied in the *two stage model* of membrane protein folding [10]. In this model, independently stable units of secondary structure (TM helices) are formed first (stage 1). These then self-assemble to form the tertiary structure (stage 2), i.e. a bundle of TM helices. This model is supported by a number of experiments on, e.g. bacteriorhodopsin. Isolated helices from bacteriorhodopsin have been shown to retain their structure when in a membrane-mimetic environment [11–13], supporting stage 1 of the model. In vitro assembly of bacteriorho-

dopsin fragments can yield functionally active protein [14–17], supporting stage 2. Thus, simulations of isolated TM helices in lipid bilayers are of relevance to stage 1 of the folding process, and simulations of helix bundles may enhance our understanding of stage 2.

In the following sections, we explore some of the background to surface associated and to transmembrane inserted helices, before going on to describe the results of recent simulation studies.

3. Helices at the bilayer surface

3.1. Membrane proteins

The X-ray structure of prostaglandin H2 synthase-1 [18] reveals that not all proteins tightly associated with a membrane contain TM helices. Instead, four amphipathic helices within the protein provide a large hydrophobic patch. The polar sides of these helices are proposed to interact with the phospholipid headgroups whilst the hydrophobic faces anchors the protein to the membrane. A similar structural motif is found in squalene cyclase [19]. Furthermore, the Pf1 phage coat protein contains a surface bound amphipathic helix in addition to a hydrophobic TM helix [20]. Thus further study of surface-oriented helices as models of such membrane proteins is justified.

3.2. Antimicrobial peptides

Many organisms possess a variety of antimicrobial defence mechanisms [21–25]. Amongst the simplest of these is induced production of small (no more than 40 residues) antimicrobial peptides. These peptides can be as short as 12 residues, are often α-helical, and form part of the animal's innate immune system. How do these small peptides exert their effect? There is an abundance of experimental data concerning such antimicrobial peptides, sometimes leading to conflicting views of their mechanisms [26–28]. Antimicrobial peptides appear to associate with the lipid headgroups of bacterial membranes. This has lead to the proposal of the 'carpet effect' [29], whereby peptides adsorbed onto the bilayer surface disrupt the packing of the lipid molecules (Fig. 2a) to such an extent that the membrane becomes leaky and the cell can no longer maintain an osmotic gradient. Solid state NMR experiments of the magainins (anti-microbial peptides found in frog skin [30]) indicate that the helices adopt an orientation parallel to the bilayer surface. This view is supported by fluorescence quenching experiments that also suggested a parallel orientation [31]. However, at higher concentrations (3.3 mol%) oriented CD spectroscopy indicated that some anti-microbial peptides (e.g. magainin and alamethicin) may be oriented perpendicular to the bilayer surface [32,33]. Furthermore, also at higher peptide:lipid ratios, large water-filled cavities within bilayers have been shown to be formed by antimicrobial peptides. Electrophysiological experiments reveal stepwise increases in ionic current across lipid bilayers on exposure to antimicrobial peptides. These have been interpreted as evidence for formation of discrete ion channels by bundles of α-helices spanning the lipid bilayer [26,34]. However, at least for those peptides that appear to interact strongly with lipid headgroups, an alternative mechanism is possible. For example, in order to explain both the formation of water-filled pores and the retention of specific interactions of peptides with lipid headgroups the formation of toroidal pores (Fig. 2b) has been proposed [33]. In this mechanism the α-helical peptide adopts a perpendicular orientation with respect to the bilayer surface but, due to local reorganisation of lipid packing, maintains close interactions with lipid headgroups along its entire length. The result is an aqueous pore, through which ions can flow, leading to cell permeabilisation and eventual death. Thus, understanding the interactions with the surface orientation is of considerable importance in characterising the mode of action of antimicrobial peptides.

3.3. The pre-pore state

3.3.1. Channel-forming peptides

Those α-helical peptides which form channels by traversing the bilayer such that the termini

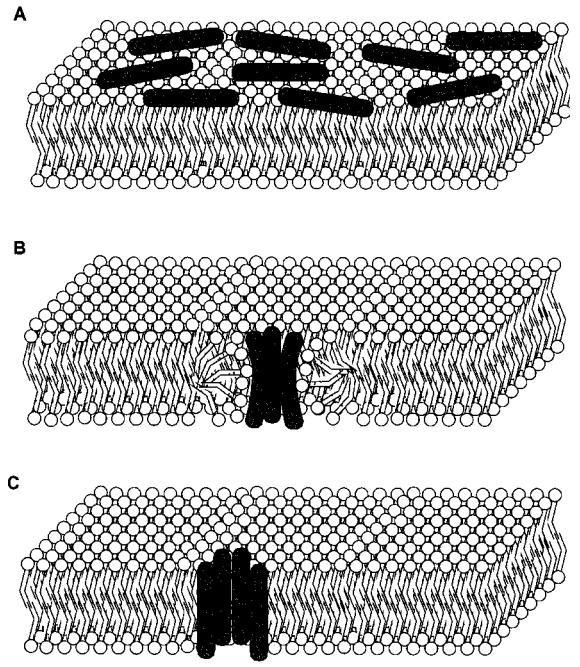

Fig. 2. (a) The carpet mechanism of membrane permeabilisation by an amphipathic α-helical peptide. Peptides are observed to adsorb onto the bilayer surface causing a disruption of the lipid headgroup packing. (b) Toroidal pore mechanism for membrane permeabilisation. Peptide sidechains interact with the lipid headgroups all along the length of the helix, promoting a local change in lipid packing. (c) The α-helix bundle model of pore-formation by channel-forming peptides. The peptides span the bilayer, their termini interacting with the lipid headgroups.

interact with the headgroups of the bilayer and the middle of the helix interacts with the acyl chains, comprise the classical view of channel-forming peptides [34,35]. This model of channel-formation (Fig. 2c) is often referred to as the 'barrel-stave' model [36]. However, in order for a channel to be formed by a bundle of TM helices, the peptide helices must first adsorb onto the bilayer surface before inserting into the bilayer to adopt a TM orientation. Indeed, it has been observed by neutron in-plane scattering that at low concentrations alamethicin (Alm) helices can adopt a surface bound orientation [37]. Thus, even for classical channel-forming peptides such as Alm, surface oriented α-helices are present in the pre-pore state.

3.3.2. Pore-forming toxins

A variety of bacterial toxins exist in both a water-soluble and a membrane-inserted state and exert their lytic effect by forming a pore in the target cell membrane [38–42]. The crystal structures of these proteins are mostly of the water soluble (i.e. pre-pore) state, and reveal them to be composed of bundles of α-helices [43]. Somehow, such proteins must undergo a major conformational change in order to form a pore in a bilayer. The proteins adsorb onto the bilayer surface where this conformational transition is initiated. This first state formed is sometimes referred to as the molten-globule state [44]. In this state the protein has increased mobility whilst retaining its secondary structural components. In particular, the α-helices of the toxins appear to remain intact, adopting a largely surface-orientation, although some pairs of helices (see below) may insert spontaneously into the bilayer [45]. Thus, once again surface oriented α-helices are important in the first stage of a cell lytic mechanism.

4. Helices spanning the bilayer

4.1. Integral membrane proteins

One of the most intensively studied integral membrane proteins (IMPs) is bacteriorhodopsin (BR), the structure of which is now known at near atomic resolution [46]. BR is a light-driven proton pump, and is made up of seven TM helices which form a tightly packed bundle within the bilayer. Thus bacteriorhodopsin is the archetype of an integral membrane protein formed by a bundle of TM helices. Such proteins range from those of electron transfer chain (e.g. cytochrome *c* oxidase [47] which contains 22 TM helices) to ion channels (e.g. the bacterial K^+ channel KcsA [48] which contains eight TM helices). The latter is of particular interest in that it illustrates how a TM helix bundle may contain within its midst a more complex structural motif. As the number of high resolution structures of membrane proteins increases it is becoming evident that the vast majority of membrane proteins are composed of TM bundles. Although the number of such structures is still relatively small, it is sufficient to allow

statistical analysis of some of the general features of their structures [49]. In addition to such a 'knowledge-based' approach, simulation studies of TM helices and TM helix bundles will help us to understand the principles of the structure and stability of proteins formed by TM helix bundles.

4.2. Channel-forming peptides

As mentioned above, channel-forming peptides generate an aqueous channel through a membrane via insertion of six or more helices to form a symmetric TM helix bundle (Fig. 3). Alamethicin (Alm) is the archetypal channel-forming peptide [35,50,51]. It is an attractive system both experimentally and for simulation studies. All the features needed to form an ion-conducting pathway across a lipid bilayer must be contained within its 20 residues. It can thus offer insight into many aspects of channel-formation and protein translocation in general, whilst serving as a model for more complex structures such as the nicotinic acetylcholine receptor [52,53].

4.3. Pore-forming bacterial toxins

As discussed above, the initial conformational change of bacterial toxins upon adsorbing to a lipid bilayer is to form a molten-globule state in which the helices are in a surface orientation. However, a subsequent key event in pore formation is the insertion of a helical hairpin into the bilayer. In, e.g. the colicins, this initial voltage independent insertion is followed by a voltage-dependent insertion/translocation movement of a large section of the pore-forming domain of the protein (68 residues) which then leads to the formation of an aqueous pore [41,54].

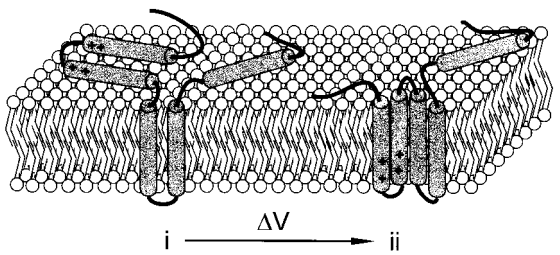

Fig. 3. Mechanism of action of an α-helical pore-forming toxin. After initial binding to the membrane surface to yield the molten globule state, there is substantial rearrangement of the protein during which a hydrophobic hairpin is believed to insert into the bilayer (i). There then follows voltage-dependent translocation (ii) of further segments which may include a second hairpin.

These bacterial toxins lend support to the more general helical hairpin hypothesis [55], which proposes that transmembrane proteins insert by means of an α-helical-hairpin. Note that such a hairpin has the most favourable alignment of the adjacent helix dipoles (although the stabilisation energy conferred by the dipole arrangement may be relatively small — see below) and most of the peptide backbone is inaccessible to the lipid environment. Thus the mechanism of action of these bacterial toxins is of general relevance to membrane protein insertion into a bilayer. This suggests that simulations of α-helix hairpin insertion into lipid bilayers will prove important.

5. The transition from surface-helix to inserted-helix

5.1. A dynamic situation

The two previous sections have indicated two extremes of the orientation of an α-helix with respect to the bilayer. It is likely that, especially for peptides, the orientation of a helix is a dynamic equilibrium between these two extremes. Various factors (e.g. peptide concentration, nature of the lipid bilayer, size and sign of a transbilayer voltage difference) may cause a shift in the position of equilibrium. The influence of a transbilayer voltage on this transition is of particular relevance to channel-forming peptides such as Alm. These peptides induce macroscopic ionic currents in a highly voltage-dependent fashion, which may be explained by voltage-induced channel formation [34,35]. A plausible theory for voltage-induced channel formation is based on the interaction of the α-helix dipole [56,57] with the transmembrane potential, ψ. The helix dipole is proposed to re-align itself with the externally imposed electrostatic field by a shift in helix orientation from surface to inserted. For the α-helix hairpins of pore-forming toxins, in which the

anti-parallel helix dipoles would cancel each other, a voltage-dependent effect is observed for the regions of protein containing charged sidechains [58].

Other factors can also influence the helix orientation equilibrium. For example, both temperature and membrane hydration influence the orientation of alamethicin and melittin [59]. At maximal membrane hydration in the fluid phase, the helices are oriented preferentially perpendicular to the membrane normal. At lower temperatures, low enough to change the phase of the lipid, the peptides were found to preferentially adopt an inserted orientation. Clearly, a number of detailed simulation studies will be needed to understand such complex interdependence of bilayer state and helix orientation.

5.2. Changes in helical conformation

Peptides in membrane-mimetic hydrophobic solvents frequently have an increased α-helical content relative to the same peptides in water [60]. Furthermore, of a number of peptides able to form amphipathic α-helices, the α-helical content increases upon interaction with the surface of a bilayer. Thus, the interaction of peptides is dynamic not only in terms of the helix orientation relative to the bilayer plane, but also in terms of the conformation (helical vs. random coil) of the peptide backbone.

This situation is further complicated by the presence of a proline in the sequences of many channel-forming peptides (e.g. Alm; melittin). An intra-helical proline often kinks the helix and may provide a molecular hinge. The possible role of proline in alamethicin has received particular attention in recent years [35,51,61]. Although the helix is significantly kinked in all three monomers of the X-ray structure, the proline hinge region could allow the peptide to more readily span the bilayer region by enabling a reduction in the kink angle thus producing a somewhat longer molecule.

Another mechanism which could enable a relatively short (≤ 20 residues) peptide to more readily span a lipid bilayer is for the peptide to adopt 3_{10} helical structure in part or all of the molecule. Indeed such 3_{10} helix formation in limited regions of the Alm molecule has been observed in NMR studies of the peptide dissolved in methanol [62]. Such a conformational change would increase the overall length of the helix.

6. Mean-field simulations

6.1. Survey of simulations

Mean-field membrane simulations provide a useful means to obtain information about possible conformations and/or orientations of a protein or peptide, whilst treating the solvent and bilayer environments as a continuum. Such models offer the advantage over all-atom simulations that they are computationally inexpensive and hence a variety of systems and comparisons can be made. They also offer the possibility of exploring long-timescale events such as conformational and/or orientational transitions. The disadvantage of such simulations is that one remains uncertain of the effects of the mean field approximations on the final results.

Mean-field simulations of helix/bilayer interactions usually employ a hydrophobicity index to represent the presence of a lipid bilayer (Fig. 4). For example, a continuum representation of a bilayer was used in early MD studies of a 46-residue segment of glycophorin [63]. The hydrophobic effect of the lipid bilayer was described by assigning an energy, h_i, to each atom which was defined as the difference in free energy of the atom in lipid and in water. This hydrophobic potential was assumed to vary along the axis parallel to the bilayer normal, with an exponential smoothing function in the interfacial region. The results of the simulation demonstrated that the insertion of a hydrophobic helix can indeed be simulated using a continuum approximation to the bilayer. This continuum model was also used in a simulation study of bacteriorhodopsin [64] which, starting from a kidney-shaped arrangement of the TM helices, successfully predicted the correct tilt of each helix with respect to the membrane.

Mean-field models are not restricted to MD simulations. For example, Monte Carlo (MC) simulations have been used to investigate the

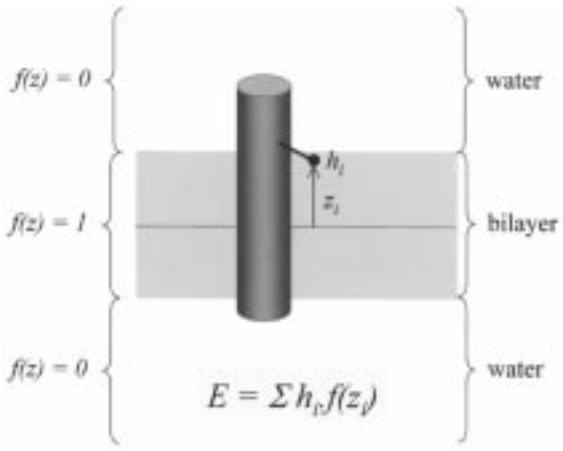

Fig. 4. A simple mean field model of the interaction of a sidechain i in an α-helix with a lipid bilayer. The sidechain is assigned a hydrophobic energy h_i (positive for hydrophilic sidechains; negative for hydrophobic), which is multiplied by a function, f, which depends on the position of the sidechain relative to the centre of the bilayer (z). The overall peptide/bilayer interaction energy is obtained by summing $h_i.f(z_i)$ over all residues.

insertion of α-helices into membranes [65]. In these studies, the protein was represented in a highly simplified fashion using a single virtual atom for each amino acid residue and the bilayer was represented in a similar fashion to that in [63]. These simulations predicted the orientation of the helices of magainin2, M2δ and melittin in agreement with experimental data. Similar studies of Pf1 bacteriophage coat protein [66] predicted a C-terminal helix traversing the bilayer with the N-terminal helix adsorbed on the surface, again in agreement with NMR data.

More recently the simple continuum model has been extended by the inclusion of a transbilayer voltage difference in the force field [67]. Simulation results showed good agreement with experimental data for a synthetic peptide from δ-endotoxin. Applying a similar approach to Alm [61] enabled development of an atomic resolution model for the voltage-dependency of channel formation. The size of the voltage applied correlated with the time taken for the peptide to first insert (Fig. 5). Furthermore, the insertion was correlated with a reduction in the kink angle, enabling the helix to more readily span the hydrophobic region.

In a further refinement of this approach, La Rocca et al. [68,69] have included a term which approximates the surface potential due to the polar groups of the lipid headgroup. To do this an all-atom model (derived from a pre-existing MD simulation of a lipid bilayer [70]) was used as the starting point for a solution of the (one dimensional) Poisson–Boltzmann equation to provide a simple continuum expression for the electrostatic potential due to the lipid headgroups and water. This model has been used in MD simulations of dermaseptin B, a frog skin antimicrobial peptide (see Table 1). The results show that the continuum representation of the bilayer stabilises an α-helical conformation of the peptide in a surface orientation, in agreement with FTIR spectroscopic studies and with subsequent all atom simulations (see below). A further refinement of this procedure, in which ionizable sidechains were modelled in their electrically neutral form when within the bilayer core, has been shown to yield an excellent correlation ($r = 0.93$) between calculated and experimental energies of helix/bilayer interactions for six synthetic peptide corresponding to helices $\alpha 2$ to $\alpha 7$ of the pore-forming domain of δ-endotoxin [71]. This latter study used a MC method to find the optimal orientation of the helices with respect to the bilayer.

Recently, the free energy of helix insertion into a bilayer has been calculated from first principles [9]. The bilayer was represented as a 30-Å slab with a dielectric constant of 2. The electrostatic and solvation components of the interaction energies of the helix with the bilayer region and with the aqueous phase were calculated on an atom by atom basis. The results indicated that a polyalanine (Ala_{25}) α-helix had two well-defined low energy orientations: one in which the helix traversed the bilayer; and a second in which the helix was on the surface of the bilayer region with its axis perpendicular to the bilayer normal. These results lend support to the earlier suggestion of Biggin et al. (1996), that inserting helices prefer to swing one end into the hydrophobic region, after first adopting a surface-bound orientation.

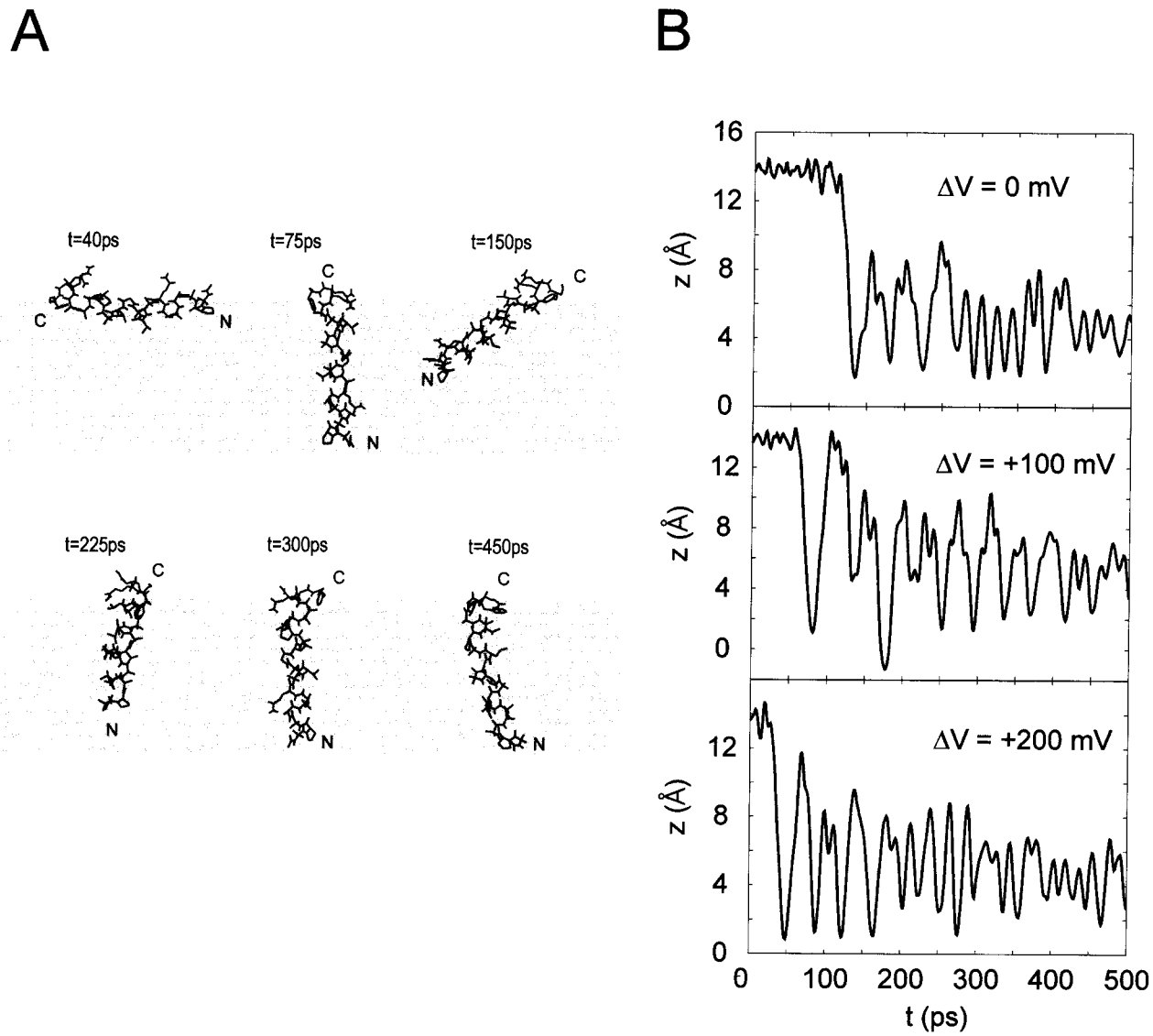

Fig. 5. Results of a mean field simulation of the interactions of an Alm helix with a bilayer [61]. (a) Snapshots from a 500-ps MD run in the presence of a bilayer and a +200-mV voltage across the bilayer. (b) Effect of a transbilayer voltage on the time taken for an Alm monomer originally positioned on the surface (at $z = 15$ Å) to insert into a bilayer. The z-coordinate of the centre of the helix is plotted vs. time for 0, +100 and +200 mV transbilayer voltages. Increasing the magnitude of the voltage decreased the time taken to insert.

Extension of these studies to a pair of Ala_{25} helices in a bilayer suggested that there was little difference in the free energies of interaction between parallel and antiparallel helix orientations, as had been suggested in earlier, somewhat more abstract, calculations [72].

Roux [73] has also investigated the inclusion of a term for the transbilayer voltage difference in mean-field models. He used the Poisson–Boltzmann equation to calculate the magnitude of free energy contributions of the transbilayer voltage for both a transmembrane helix and for an embedded membrane protein. For the case of the TM helix with a transbilayer voltage difference of

Table 1
Sequences of helices (part 1)

Peptide toxins	
Alamethicin	Ac-Aib-Pro-Aib-Ala-Aib-Ala-Gln-Aib-Val-Aib-Gly-Leu-Aib-Pro-Val-Aib-Aib-Glu-Gln-Phol
Melittin	Gly-Ile-Gly-Ala-Val-Leu-Lys-Val-Leu-Thr-Thr-Gly-Leu-Pro-Ala-Leu-Ile-Ser-Trp-Ile-Lys-Arg-Lys-Arg-Gln-Gln-NH_2
Magainin	Gly-Ile-Gly-Lys-Phe-Leu-His-Ser-Ala-Lys-Lys-Phe-Gly-Lys-Ala-Phe-Val-Gly-Glu-Ile-Met-Gln-Ser
Dermaseptin-B	Ala-Met-Trp-Lys-Asp-Val-Leu-Lys-Lys-Ile-Gly-Thr-Val-Ala-Leu-His-Ala-Gly-Lys-Ala-Ala-Leu-Gly-Ala-Val-Ala-Asp-Thr-Ile-Ser-Gln
De novo synthetic peptides	
LS2	Leu-Ser-Leu-Leu-Leu-Ser-Leu-Leu-Ser-Leu-Leu-Leu-Ser-Leu-Leu-Ser-Leu-Leu-Leu-Ser-Leu
LS3	Leu-Ser-Ser-Leu-Leu-Ser-Leu-Leu-Ser-Ser-Leu-Leu-Ser-Leu-Leu-Ser-Ser-Leu-Leu-Ser-Leu
Peptide 16	Lys-Lys-Gly-Leu-Leu-Leu-Leu-Leu-Leu-Leu-Leu-Leu-Leu-Leu-Leu-Leu-Leu-Leu-Leu-Leu-Lys-Lys-Ala
Peptide fragments of single TM helix proteins	
Pf1[a]	Met-Leu-Ala-Ile-Gly-Gly-Tyr-Ile-Val-Gly-Ala-Leu-Val-Ile-Leu-Ala-Val-Ala-Gly-Leu-Ile-Tyr-Ser-Met
Influenza A M2	Ser-Ser-Asp-Pro-Leu-Val-Ile-Ala-Ala-Ser-Ile-Ile-Gly-Ile-Leu-His-Phe-Ile-Leu-Trp-Ile-Leu-Asp-Arg-Leu-Phe
Influenza B NB	Ser-Ile-Ile-Ile-Thr-Ile-Cys-Val-Ser-Leu-Ile-Val-Ile-Leu-Ile-Val-Phe-Gly-Cys-Ile-Ala
HIV-1 Vpu	Ile-Val-Ala-Ile-Val-Ala-Leu-Val-Val-Ala-Ile-Ile-Ile-Ala-Ile-Val-Val-Trp-Ser-Ile-Val-Ile-Ile
Glycophorin	Ile-Thr-Leu-Ile-Ile-Phe-Gly-Val-Met-Ala-Gly-Val-Ile-Gly-Thr-Ile-Leu-Leu-Ile-Ser-Tyr-Gly-Ile
Peptide fragments of multiple TM helix proteins	
Bacteriorhodopsin	
Helix A	Trp-Ile-Trp-Leu-Ala-Leu-Gly-Thr-Ala-Leu-Met-Gly-Leu-Gly-Thr-Leu-Tyr-Phe-Leu-Val-Lys-Gly-Met
Helix B	Asp-Ala-Lys-Lys-Phe-Tyr-Ala-Ile-Thr-Thr-Leu-Val-Pro-Ala-Ile-Ala-Phe-Thr-Met-Tyr-Leu-Ser-Met-Leu-Leu
Helix C	Trp-Ala-Arg-Tyr-Ala-Asp-Trp-Leu-Phe-Thr-Thr-Pro-Leu-Leu-Leu-Leu-Asp-Leu-Ala-Leu-Leu
Helix D	Ile-Leu-Ala-Leu-Val-Gly-Ala-Asp-Gly-Ile-Met-Ile-Gly-Thr-Gly-Leu-Val-Gly-Ala-Leu
Helix E	Trp-Trp-Ala-Ile-Ser-Thr-Ala-Ala-Met-Leu-Tyr-Ile-Leu-Tyr-Val-Leu-Phe-Phe-Gly-Phe-Thr
Helix F	Val-Ala-Ser-Thr-Phe-Lys-Val-Leu-Arg-Asn-Val-Thr-Val-Val-Leu-Trp-Ser-Ala-Tyr-Pro-Val-Val-Trp-Leu-Ile
Helix G	Ile-Glu-Thr-Leu-Leu-Phe-Met-Val-Leu-Asp-Val-Ser-Ala-Lys-Val-Gly-Phe-Gly-Leu-Ile-Leu-Leu-Arg
Nicotinic receptor	
Helix M2 δ	Glu-Lys-Met-Ser-Thr-Ala-Ile-Ser-Val-Leu-Leu-Ala-Gln-Ala-Val-Phe-Leu-Leu-Leu-Thr-Ser-Gln-Arg
Voltage gated K^+ channel	
Helix S5	Ser-Met-Arg-Glu-Leu-Gly-Leu-Leu-Ile-Phe-Phe-Leu-Phe-Ile-Gly-Val-Val-Leu-Phe-S er-Ser-Ala-Val-Tyr-Phe-Ala-Glu
Helix S6	Phe-Trp-Gly-Lys-Ile-Val-Gly-Ser-Leu-Cys-Val-Val-Ala-Gly-Val-Leu-Thr-Ile-Ala-Leu-Pro-Val-Pro-Val-Ile-Val-Ser-Asn-Phe-Asn
Bacterial K^+ channel	
Helix M1	Leu-His-Trp-Arg-Ala-Ala-Gly-Ala-Ala-Thr-Val-Leu-Leu-Val-Ile-Val-Leu-Leu-Ala-Gly-Ser-Tyr-Leu-Ala-Val-Leu-Ala-Glu
Helix M2	Leu-Trp-Gly-Arg-Leu-Val-Ala-Val-Val-Val-Met-Val-Ala-Gly-Ile-Thr-Ser-Phe-Gly-Leu-Val-Thr-Ala-Ala-Leu-Ala-Thr-Trp-Phe

[a] Only the sequence of the TM helix is given, even though simulations [129] included the entire sequence.

100 mV, the contribution of the voltage difference to the interaction energy is of the order of 1 kcal/mol. This is about the same as from a simple calculation of the energy of a helix dipole (63 debye) in a linear transbilayer electrostatic field (100 mV/30 Å) [34,74]. The results for a spherical representation of a membrane protein showed that the energetics of charges inside the protein will be affected by both their transverse and lateral positions relative to the centre of the sphere. This implies that charge movements do not have to take place solely in the direction of the membrane normal in order to experience the transbilayer voltage. This has important implications for the S4 voltage sensor helix of voltage-gated ion channels. For the voltage-gated ion channels there is experimental evidence for a voltage-induced movement of this helix [75,76]. These calculation suggest that one cannot make simple assumption a priori of the direction in which this movement occurs.

The mean-field approach has also been applied to helix hairpins. Using MC simulations [77] it has been shown that the insertion process of helical hairpins follows a well-defined pattern of kinetic steps. In particular, this work shows how the anisotropic orientational order and lateral density fluctuations affect protein insertion and hairpin formation. In these simulations, the protein was modelled in the same manner used by Milik and Skolnick [65], whilst the lipid was modelled as monolayer of hard parallel cylinders. This represents an intermediate between a continuum model of a bilayer and an all atom representation. It was found that the lateral compression of the 'lipids' leads to exclusion of the hairpin loop at the trans side of the membrane. If the 'lipids' were omitted from the simulation, the protein was found to be less stable and hairpins did not form.

6.2. Conclusions and directions

The use of continuum simulations for the study peptide/bilayer interactions offers a practical means for qualitative prediction of the behaviour of such systems. Such methods are useful where all-atom simulations are computationally too expensive. Many, if not all, of the continuum representations of a lipid bilayer depend on an interpretation of the hydrophobic effect due to the lipid bilayer. This has lead to many different scales and viewpoints [78,79]. A major drawback to the use of such scales is that it is difficult to account for inter- and intra-helix charge–charge interactions. Thus, even though charged TM helices are known to exist within membranes [80], the commonly used scales would underestimate their hydrophobicity and would tend to position them outside the lipid region. However, recent work [81] has offered insights into the stabilisation offered by such interactions and their effects on peptide stability both inside a lipid bilayer and also within the interior of a soluble protein.

Continuum models are still evolving in an attempt to reproduce different aspects of helix/bilayer interactions in a computationally efficient manner. The studies discussed above have revealed some success with simple models of hydrophobic interactions and of the dipole and transmembrane electrostatic potentials. However, substantial challenges remain, including the variation in dielectric constant across a bilayer and the effective viscosity of the lipid environment.

7. All atom simulations

7.1. Detailed MD simulations

In addition to simulations in which the lipid bilayer is represented as a continuous mean field, it is possible to run simulations in which both the lipid molecules and the water on either side of the membrane are represented atomistically. Such simulations of α-helix/bilayer interactions exploit the considerable progress over the past few years in simulations of lipid bilayers per se [3–6]. Such studies have explored the dependence of predicted structural and dynamic properties of bilayers on the methods employed, and have established 'rules of thumb' for physically realistic bilayer simulations, in terms both of suitable parameters for inter-atomic interactions, and of optimal protocols (e.g. *NVE* vs. *NPT* conditions).

In addition to extending simulations of pure lipid bilayers, full bilayer simulations of α-helix/bilayer interactions also benefit from de-

tailed simulation studies of α-helical membrane-derived peptides in various solvent environments. For example, simulations of the integral membrane helix of surfactant protein C in methanol, chloroform and water have been used to compare its stability in these different environments [82]. These simulations revealed that the α-helix remained stable over a period of 1 ns in water and in methanol, and in particular showed that a cluster of valine residues in the sequence did *not* destabilise the helix, despite the low helix propensity of β-branched sidechains in water-soluble proteins [83]. This parallels experimental studies of Deber [84,85] which have indicated that β-branched sidechains are favourably accommodated within an α-helix when the latter is in a membrane-mimetic environment. Likewise, Dempsey and colleagues have performed MD simulations of the channel-forming peptides alamethicin and melittin [86] in methanol, comparing the simulation results with NMR amide exchange data.

By combining these two approaches there have been a number of simulations of α-helices in the presence of explicit lipid plus water molecules. These are reviewed in the following sections. Such studies also follow on from earlier simulations [87] of the tripeptide Ala-Phe-Ala-O-*t*Bu at the surface of a DMPC bilayer.

What are the aims and objectives of atomistic simulations of α-helices in bilayers? Firstly, they enable atomic resolution characterisation of the interactions of α-helical peptides with their water and phospholipid environment. This is of particular importance in terms of understanding, e.g. how TM α-helices interact with the complex environment in the 'interfacial' region between the bulk aqueous phase and the hydrophobic core of the bilayer. As we have seen, an accurate model of such interactions is one of the major challenges facing mean field simulations. The second objective of full bilayer simulations is to characterise the structural dynamics of α-helices in their membrane environment. As discussed above, current mean field models do not model, e.g. the effective 'viscosity' of the hydrophobic bilayer core. This is likely to have an influence on, e.g. the dynamics of bending of TM α-helices about proline-induced 'hinges'.

It is important to remember that there are limitations to MD simulations of α-helices in a full bilayer environment. To a large extent these are the same as the current limitations of such simulations for pure bilayers. Long range electrostatic interactions are generally treated in a somewhat approximate fashion, e.g. via the use of simple cutoffs. Further work is needed to evaluate the use of, e.g. Ewald summation techniques to better treat such long range interactions in bilayer simulations. The durations of bilayer simulations (realistically of the order of 1–10 ns with current programs and computers) are relatively short compared with the relaxation rates of the lipids [6]. Consequently, good mixing/equilibration of lipid and peptide is difficult to achieve. Thus, mean field simulations may play a role in generating initial configurations for subsequent atomistic simulations. Finally, most simulations neglect the ionic environment in the aqueous phases or the voltage difference across the bilayer, both of which are present for most cell membranes.

In the following sections we will review full bilayer simulations, starting with studies which have employed approximations to a full bilayer, then looking at single TM α-helices in a full bilayer environment, before considering more complex systems in a full bilayer, such as α-helices at the bilayer surface and bundles of α-helices.

7.2. 'Simplified' bilayers and helices

A number of simulation studies have employed a simplified atomistic model of a bilayer, i.e. a situation midway between a mean field representation and a full model of all of the phospholipid atoms. An early study applied this approach to simulate poly-glycine and glycophorin TM α-helices embedded in a bilayer mimic of approx. 50 DPPC molecules [88]. Explicit water molecules were not included, and the lipid headgroups were left uncharged. The integrity of the bilayer was maintained by harmonic planar restraints on the headgroups. During a 50-ps simulation, the back-

bone of glycophorin was found to retain an α-helical conformation.

More recently, Klein and colleagues have used an octane 'slab' between two aqueous phases as a mimic of the environment provided by the hydrophobic core of a lipid bilayer. (A similar approach has been used by Pohorille and colleagues [89]; see below.) This membrane-mimetic environment has been used in two MD simulations of ion channels formed by bundles of α-helices, the peptides being synthetic peptides designed de novo by DeGrado and colleagues [90,91]. The first study [92] explored four-helix bundles of the LS2 peptide (see Table 1), which form proton permeable pores [90]. The helix bundle model started off as four exactly parallel, ideal α-helices, oriented such that their polar sidechains pointed towards the interior of the pore. After 4 ns of unrestrained MD simulations, these helices had evolved into a coiled-coil tetrameric structure with a left-handed twist. Interestingly, such a structure had been proposed earlier on the basis of restrained in vacuo MD simulations which omitted any model of the bilayer [93,94]. This suggests that TM helix bundle models may be constructed by less costly simulations without a bilayer, and then refined by subsequent MD simulations in an atomistic bilayer or bilayer-mimetic environment.

In a subsequent study [95] similar simulations were performed for hexameric parallel bundles of the LS3 (see Table 1) peptide, which correspond to monovalent cation selective channels [90]. These were found to form unstable bundles, irrespective of whether the simulation was started from exactly parallel helices or from a coiled-coil model. Significantly, when a transbilayer voltage term was included in the simulation (in a manner similar to that employed earlier [61] in mean field simulations of Alm/bilayer interactions — see above), the hexameric helix bundle was stabilised. This provides an interesting correlation with experimental data on the voltage-dependent formation of LS3 channels. However, it remains to be seen whether such hexameric helix bundles would be stable in the absence of a transbilayer voltage if the bilayer-mimicking octane slab was replaced by a full lipid bilayer, including polar lipid headgroups.

Recently, the same approach with a bilayer-mimetic octane slab has been applied to models of a putative ion channel [96] formed by a bundle of five TM α-helices from the Vpu protein of HIV-1 [97]. In this study the authors observe that initial models similar to that generated by restrained in vacuo MD simulations [98] are unstable in the bilayer mimicking simulation. Instead, they propose a model in which the tryptophan residues of the TM helices are directed towards the centre of the pore. However, it should be remembered that these simulations do not include a proper model of the lipid/water interface or lipid headgroups. As both experimental [99–101] and simulation ([102–104]; also see below) results suggest that tryptophan sidechains prefer an interfacial location and may make H-bonding interactions with lipid oxygen atoms in this region, one wonders whether the instability of the Vpu pore model in the octane slab environment might simply reflect the absence of such interactions. The octane slab method has also been applied to the influenza M2 ion channel [105] (see below).

A further simulation which might be considered as a bilayer-mimicking simulation is that of Woolf on the glycophorin TM helix dimer in dodecylphosphocholine micelles [106]. This work is of particular interest, as the dynamics of the TM helix dimer in a micelle, in a bilayer and in water have been compared. Micelles are often used a membrane-mimetic environment in NMR studies of TM helices [107].

7.3. TM helices in full bilayers

There have been a number of simulations of TM helices in a fully solvated bilayer environment. These range from simulations of simple model helices, to studies of TM helices taken from integral membrane proteins.

Stouch and colleagues performed an extended (>1 ns) MD simulation of an Ala_{32} α-helix spanning a DMPC bilayer [108]. This highly simplified model of a hydrophobic TM helix exhibited surprisingly rich behaviour. As one might have anticipated, the central 12 residues of the peptide formed a very stable α-helical core. Regions of

the peptide either side of this core interacted with lipid headgroups and with interfacial water molecules, exhibiting increased conformational variability whilst remaining predominantly helical. The N- and C-termini of the peptide chain were fully exposed to water and adopted random coil conformations. Unexpectedly, given the simple sequence of the peptide, the helix exhibited a tendency to kink at the centre of the bilayer. Thus, even with a highly simplified TM sequence structural heterogeneity was observed, corresponding to the anisotropy of the environment along the bilayer normal.

A somewhat more complex peptide model (peptide-16; see Table 1) has been studied in MD simulations in which the TM helix was surrounded by 12 DMPC molecules (six in each layer) and the resultant system was solvated with approx. 600 water molecules, using hexagonal periodic boundary conditions (PBCs) to generate a bilayer [109]. As in an earlier simulation of a gramicidin A dimer in a DMPC bilayer [110] the lipid molecules surrounding the α-helical peptide were taken from a pre-existing library of 2000 different lipid conformations. Peptide-16 is an attractive simple model of a TM helix in that it contains a hydrophobic core with polar sidechains present at either end of the helix in the regions which lie within the lipid/water interfacial region of the bilayer. During the course of the 1-ns simulation the α-helical conformation of the peptide was largely maintained, although distortions at the ends of the helix were seen, and a slight bend appeared midway through the simulation. The lysine sidechains at either end of the helix were well hydrated by waters in the interfacial region. Interestingly, over the 1 ns period, the lysine sidechains did not show any significant mobility, whereas (some of) the leucine sidechains showed multiple χ_1 and χ_2 dihedral angle transitions. This suggests relatively long-lasting patterns of sidechain H-bonding interactions in the interfacial region, in contrast with relatively fluid hydrophobic interactions in the bilayer core.

A similar simulation strategy was used to examine the dynamics of all seven of the individual TM helices from bacteriorhodopsin in a DMPC bilayer [111]. Again, each helix was surrounded by a bilayer of 12 phospholipid molecules. For helices B, C and D, simulations with ionizable sidechains in both their charged and uncharged forms were performed. Significantly, this study revealed differences in motional behaviour between the different α-helices. In particular, the absence of aromatic residues from the 'interfacial' region or the presence of a proline residue within a helix enhanced its mobility. A further interesting result concerned Ser and Thr sidechains within the helices. Previously, on the basis of analysis of X-ray structures of these sidechains in the helices of globular proteins [112] it had been suggested that in TM helices Ser and Thr sidechains would satisfy their H-bonding potential by forming H-bonds back to the $(i-3)$ and $(i-4)$ mainchain carbonyl oxygen. However, in these simulations such sidechains when in the hydrophobic core frequently did *not* form such H-bonds. In a subsequent paper analysing these simulations in more detail [113], the interaction energies with the bilayer of amino acids within the TM helices were compared with the widely used GES scale for hydrophobicities [114]. Interestingly, the most marked deviations of the MD derived interaction energies from the GES scale was for the aromatic sidechains. This was due to the especially favourable interactions these residues could make at the bilayer/water interface. In particular, Trp and Tyr sidechains were able to form favourable H-bonds to lipid and to water when in this region. This had previously been observed for Trp sidechains in simulations of gramicidin in DMPC [110].

The above simulations have employed an 'annulus' of phospholipid around the TM helix, 'multiplied' by PBCs. A number of recent simulations have employed a more extensive bilayer (e.g. approx. 128 phospholipid molecules instead of 12), again with PBCs. Thus these latter simulations correspond to a lower peptide:lipid ratio, and are thus closer to many experimental situations. These more recent studies employ the same protocol as that adopted in a landmark simulation of the OmpF porin trimer in a full lipid bilayer plus water environment [115]. A simulation of a TM Alm helix in a POPC bilayer (a total of approx. 17 000 atoms including water) [116] compared the

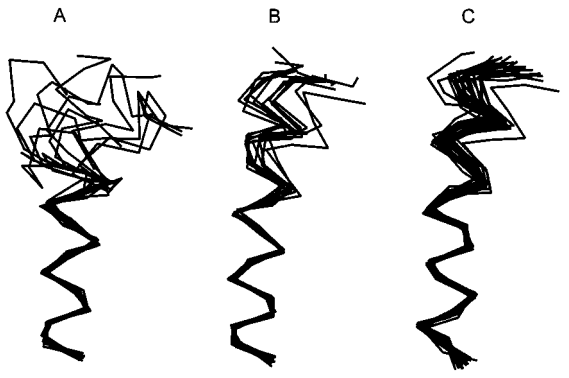

Fig. 6. Ca traces, corresponding to structures saved every 100 ps, for simulations of an Alm helix: (a) in water; (b) in MeOH; and (c) inserted across a POPC bilayer [116]. The structures were superimposed using their N-terminal helices (residues 1–11). The N-termini are at the bottom of the diagram.

conformational dynamics of the TM peptide with those of Alm in solution in either MeOH or water. In the bilayer and in methanol, there was little change from the initial helical conformation of the peptide (Cα RMSDs of approx. 0.2 nm over 2 ns and 1 ns for the bilayer and MeOH simulations, respectively). In water there were substantial changes (a Cα RMSD of approx. 0.4 nm over 1 ns), especially in the C-terminal segment of the peptide which lost its α-helical conformation (Fig. 6). In the bilayer and in MeOH, the Alm molecule exhibited hinge-bending motion about its central Gly–X–X–Pro sequence motif. Analysis of H-bonding interactions suggested that the polar C-terminal sidechains of Alm formed multiple H-bonds in the bilayer/water interface region which persisted throughout the simulation. This correlates well with the preferred mode of helix insertion into the bilayer via insertion of the N-terminus of the Alm helix, which is believed to underlie the asymmetry of voltage activation of alamethicin channels, as was also observed in mean field simulations of Alm/bilayer interactions ([61]; see above).

All of the above simulations involve either peptides or TM helices isolated from membrane proteins for which the three dimensional structure is known. However, the great majority of membrane proteins, although containing one or more TM helices [1], are of unknown three dimensional structure. Several algorithms exist for prediction of the number and position of TM helices within a membrane protein sequence [117–121]. However, these methods tend to disagree over the beginning and end residues of TM helices, posing problems for subsequent modelling and simulation studies. MD simulations of model TM helices may be used to refine the results of such prediction. This has been explored for the TM helix of the M2 protein from influenza A virus [104]. M2 is a small protein, 97 amino acids long, which contains a single TM segment towards the N-terminus of its polypeptide chain (Table 1). In cell and virus membranes the protein tetramerises to form proton permeable ion channels. Based on comparison of the results of five different secondary structure prediction algorithms 18-, 26- and 34-residue M2 TM helices were simulated. Each simulation system contained 127 POPC molecules plus from approx. 3500 to 4700 waters, and the total simulation time amounted to 11 ns. Analysis of time dependent secondary structure of the TM segments enabled identification of those residues which adopted a stable α-helical conformation throughout the simulation. In this way a core TM region of approx. 20 residues was defined. Polar sidechains, including a tryptophan, on either side of this region form relatively long-lived H-bonds to lipid headgroups and water molecules in the water/bilayer interface (Fig. 7). More recently, this approach has been applied to related viral channel proteins, such as NB from influenza B and Vpu from HIV-1 [122,123].

A similar approach has been applied to the pore-lining TM helices of two K^+ channels, KcsA (a bacterial channel, the three dimensional structure of which is known at 3 Å resolution [48]) and Shaker (a homologous eukaryotic channel) [124]. All four pore-lining helices (M1, M2, S5 and S6; see Table 1) were simulated for 1 ns in a POPC bilayer. The outer pore-lining helices (M1 in KcsA and S5 in Shaker) tended towards a slightly more curved geometry, as is observed for M1 in the X-ray structure of KcsA. The inner pore-lining helices (M2 in KcsA and S6 in Shaker), appeared to be somewhat more flexible than the outer pore-lining helices. In particular, the Pro–Val–

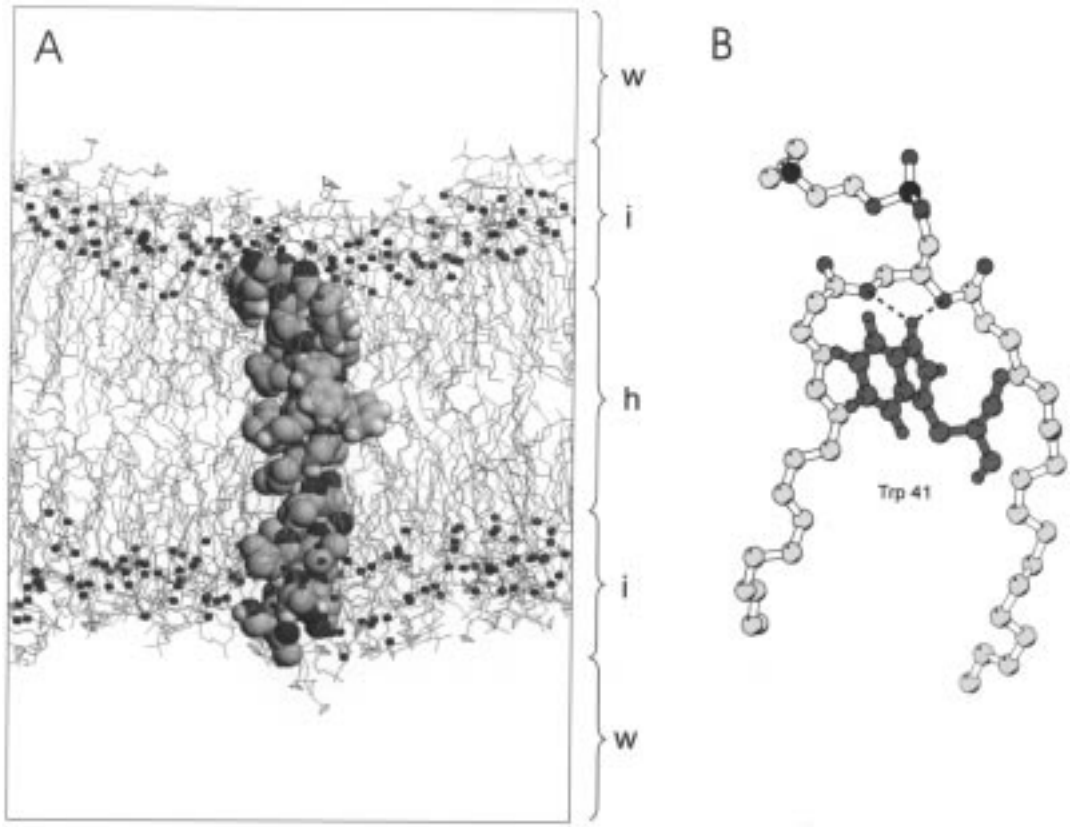

Fig. 7. (a) Snapshot of the simulation system for a 26-residue model of the influenza A M2 helix spanning a POPC bilayer. The water molecules are omitted for clarity. The peptide atoms are shown in space-filling format, and the carbonyl oxygens of the phospholipid molecules as small dark grey spheres. The approximate extents of the water (w), interfacial (i) and hydrophobic core (h) regions of the system are indicated. (b) Snapshot of a long-lasting H-bond an M2 helix sidechain (Trp41) and the two ester oxygens of a lipid molecule (results from [104]).

Pro sequence motif of S6 resulted in flexibility about a central hinge, as was suggested by previous in vacuo simulations [125]. It was suggested that such 'hinge-bending' motion of M2 might be related to the gating mechanism of the channel [126]. Aromatic residues at the extremities of the helices underwent complex motions on both short (< 10 ps) and long (> 100 ps) timescales.

Overall, these studies have shown that MD simulations of single TM helices in an atomistic bilayer environment are feasible, and that they can yield information concerning helix dynamics and the nature of peptide/bilayer/water interactions. The future direction for such simulations will lie in their extension to biologically important problems, such as aiding the prediction of membrane protein structures and casting a light on possible gating mechanisms of ion channels.

7.4. Surface helices

All of the above peptide/bilayer MD simulations have been of TM helices, in which only residues at either end of the helix experience the complex interfacial environment. However, as discussed above, α-helices located at the surface of a bilayer are also of great biological importance. At least half, if not all, of the sidechains of such helices experience an 'interfacial' environment. Simulations of surface helices are rather more difficult, if only because one is often uncertain exactly where to position such helices relative to

the centre of a bilayer. There are two approaches to this problem. One is to exploit available experimental data to arrive at a 'best guess' of how deeply into a bilayer a given surface-located helix penetrates. The second is to carry out a systematic series of simulations which probe the behaviour of the system for different locations of the surface helix.

Before considering simulations of α-helices at the surface of a bilayer, it is useful to consider a number of related simulations that provide some insight into the complexities. A series of simulations using a water liquid/vapour interface as a simple model of a water/hydrophobic interface have been performed [89] in order to mimic peptide folding at a membrane surface. These used the simple heptapeptide sequence LQQLLQL, which has the potential to form an amphipathic α-helix. Two simulations started with this peptide at the interface, in either an α-helical or a β-strand conformation. The α-helical peptide oriented itself so that the Q residues pointed into the water and the L sidechains into the vapour. This conformation was retained throughout the 3-ns simulation. Starting from a β-strand conformation (which does not allow this peptide to form an amphipathic structure) a number of torsion angles within the peptide underwent a $\beta \rightarrow \alpha$ transition during a 15-ns simulation. Although the interfacial environment has been radically simplified, this study is of importance in that it demonstrates that simulations can be used to explore aspects of conformational stabilisation of peptides at a bilayer surface.

A simplification of the bilayer surface was also made in simulations of the lipid-degrading enzyme phospholipase A_2 [127]. In these simulations, the bilayer was approximated by a DLPE *monolayer* of 101 lipid molecules. Two monolayer/enzyme complexes were simulated, each for 120 ps: a loose complex, and a tight complex, differing in the initial position of the protein molecule (which was docked manually onto the lipid surface). This illustrates one of the difficulties of such studies, i.e. that of deciding upon the initial position of the protein relative to the bilayer. The lipids involved in contacts with the protein were shown to be desolvated in the tight complex, but not in the loose complex. The desolvated lipid molecules interacted mainly with hydrophobic amino acid sidechains.

Turning to simulations of amphipathic α-helices at a bilayer surface, the first such study was a 500-ps MD simulation of an amphipathic α-helical peptide fragment of corticotropin-releasing factor at the surface of a bilayer of 60 DOPC molecules [128]. This suggested that the helical conformation of the peptide was stabilised by interactions with the bilayer, although as the comparison was made with an in vacuo simulation of the same peptide the degree of stabilisation was difficult to establish.

Roux and Woolf [129] examined the 46-residue viral coat protein Pf1, which forms an integral membrane protein with an N-terminal amphipathic α-helix (residues 6–13) at the bilayer surface and a C-terminal (residues 19–42) hydrophobic α-helix which spans the bilayer. A model of the protein based on a combination of NMR data and simple conformational searching was simulated in the presence of a bilayer of 33 DPPC molecules and 1308 waters for 200 ps, using hexagonal PBCs. This simulation was most interesting in terms of what it revealed of the interactions of the amphipathic, surface-bound helix with the lipid/water interface. Radial distribution functions of side chain atoms in the amphipathic helix showed that only the polar sidechains were exposed to water. Furthermore, both tyrosine residues (Y25 and Y40) in the protein were located in an interfacial region. The hydroxyl group of Y25 formed an H-bond to water, whilst that of Y40 formed an H-bond to the ester carbonyl of a DPPC molecule, again confirming the importance of the complex interfacial environment in the interactions of amphipathic aromatic sidechains.

A similar approach has recently been applied to melittin [130] in which the initial configuration of the system was such that although the overall helix axis was approximately parallel to the bilayer plane, the helix kink (induced by the central proline) resulted in the N-terminus of the helix penetrating deep into the core of the bilayer. This resulted in significant local perturbation of the bilayer structure and penetration of water through

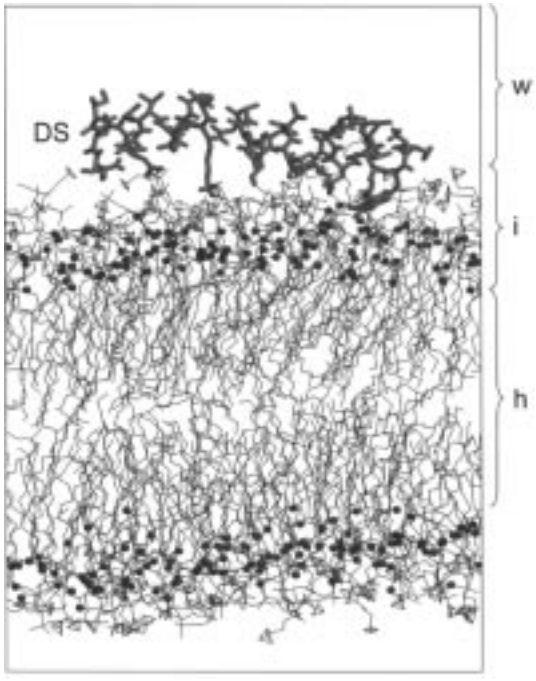

Fig. 8. Snapshot at the end of a 2-ns MD simulation of dermaseptin-B (DS) bound to the surface of a POPC bilayer. Other details as for Fig. 7.

the leaflet of the bilayer opposite to that to which melittin was bound. This was suggested to be related to the mechanism of membrane lysis of this peptide. It will be interesting to see how simulation studies may be used to characterise the transition from aqueous phase melittin to surface-adsorbed peptide to the location in these simulations.

A series of MD simulations of dermaseptin B (a membrane disrupting peptide from frog skin; see above) at the surface of a bilayer of 128 POPC molecules have been performed [131] (La Rocca and Sansom, in preparation). The 'docking' of the peptide helix with the bilayer surface was achieved using a 500-ps MD run during which the helix was slowly moved towards the bilayer surface, allowing the lipid molecules to 'relax' around it. Following this, a 2-ns MD run was performed. Thus, the starting configuration of the production run of the MD simulation corresponded to a 'surface bound' helix rather than to a more deeply penetrating orientation as in the melittin simulation discussed above. The results revealed considerable stabilisation of the α-helical conformation of the surface-bound form of the peptide (Fig. 8), compared to the same molecule when simulated in water for 2 ns. The sole tryptophan residue (Trp3) residue of the molecule formed H-bonds to both water and to a phosphate oxygen of a lipid molecule. Thus, the simulation of dermaseptin B in an explicit lipid bilayer and water environment produced a good correlation with the results of both experimental studies and of the mean-field simulations (see above; [69]).

Overall, these studies have demonstrated that atomistic simulations of surface-bound α-helices are feasible, and suggest that they may reveal useful information on how such helices are stabilised at the 'interface', and as to possible mechanisms of action of membrane-perturbing peptides. However, it is evident that the initial setup of such simulations is non-trivial. A number of systematic studies are needed to establish to what extent the behaviour in the subsequent simulation run is determined by the assumptions made as to the position of the helix relative to the bilayer surface.

7.5. α-Helix bundles

The simulations discussed so far have been concerned with the stability and interactions of isolated TM helices at the surface of or spanning lipid bilayers. Such simulations provide atomic resolution information on the nature of helix/bilayer interactions. This is important in the context of the two stage model of membrane protein folding [10] which proposes that TM helices are in themselves stable in a bilayer environment, and subsequently pack together to form a helix bundle. However, it is important to remember that TM helices will find themselves in an even more complex environment when they form part of a helix bundle (i.e. an integral membrane protein). There have been a limited number of simulation studies of TM helix bundles using an atomistic lipid bilayer plus and solvent environment.

An impressive early study of an intact helix bundle protein in a lipid bilayer is [132], which describes an MD simulation of a bacteriorho-

dopsin trimer in the presence of 30 lipid (diphytanylphosphatidyl glycerophosphate) molecules plus water molecules and counterions. By the end of the 300-ps duration of the simulation the Cα RMSD was approx. 2.5 Å from the initial structure for bacteriorhodopsin. The fluctuations of the inter-helix loops and of the ends of the helices were, as might be anticipated, greater than those of the helix cores. Analysis of 12 internal water molecules inside the helix bundle revealed several stable water positions. However, most of internal waters exchanged with bulk water during the simulation.

More recently, full bilayer simulations have been extended to two simple models of ion channels formed by α-helix bundles, namely Alm and influenza M2. Studies on Alm initially focused on a hexameric helix bundle in a bilayer of approx. 120 POPC molecules (Fig. 9) [133], and more recently have been extended to simulations of bundles with $N = 5$, 6, 7 and 8 helices [134]. Simulation times ranged from 1 ns ($N = 5$, 7 and 8) to 2 ns (although all four simulations have since been extended to 4 ns — Sansom and Tieleman, unpublished results). The results of 2 ns simulations of a hexameric bundle of Alm

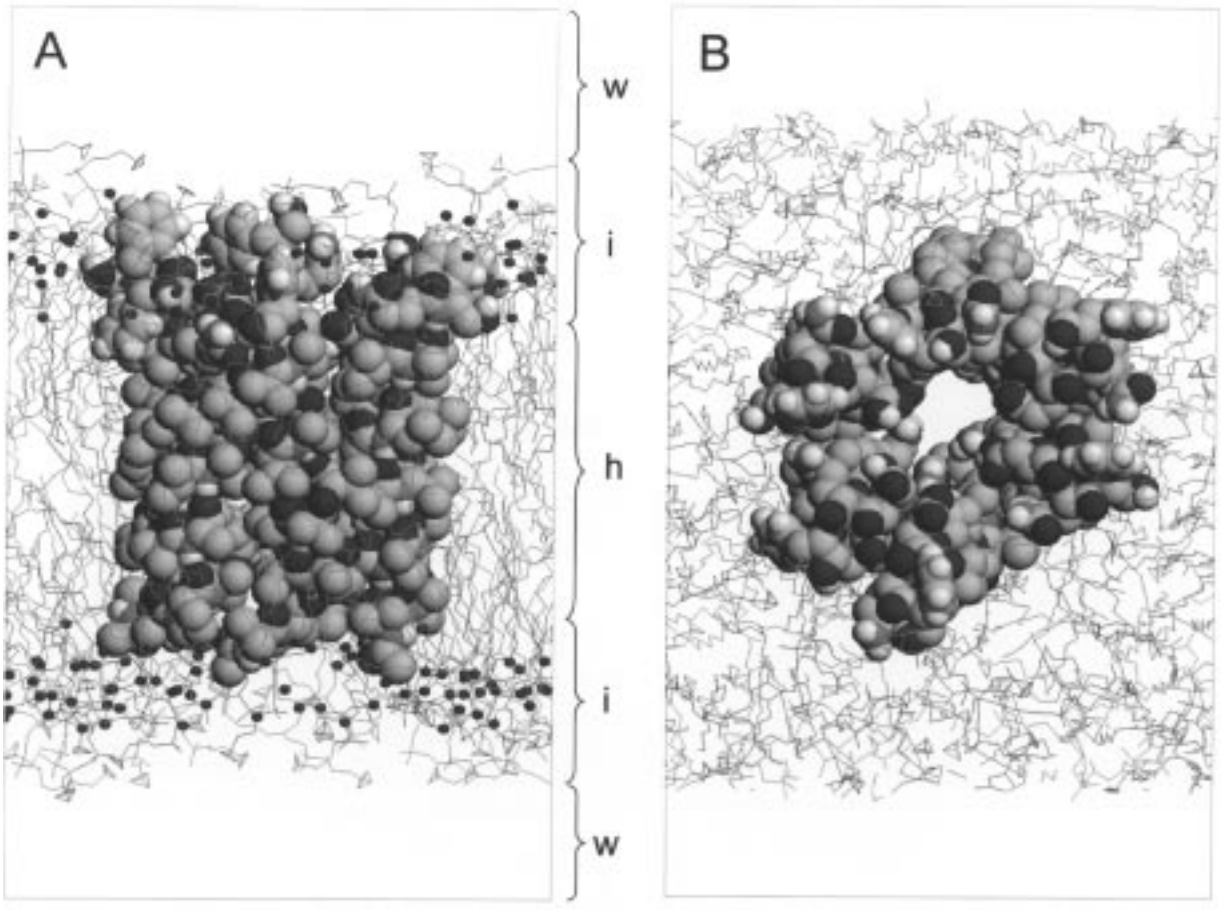

Fig. 9. Images of an $N = 6$ Alm α-helix bundle simulation in a POPC bilayer, taken at $t = 4$ ns. The peptide atoms are shown in space-filling format, and the carbonyl oxygens of the phospholipid molecules as small dark grey spheres. (a) View perpendicular to the pore axis, with the C-terminal mouth of the pore uppermost. (b) View down the pore (z) axis, with the C-terminal mouth of the pore towards the reader.

helices in a POPC bilayer explored the dynamic properties of this model of a helix bundle channel, and also investigated the effects of changing ionisation state of the ring of Glu18 sidechains on bundle stability. If all of the Glu18 sidechains were ionised, the bundle was unstable; if none of the Glu18 sidechains was ionised the bundle was stable. The structural and dynamic properties of water in this model channel were examined. As in earlier in vacuo simulations [135] the dipole moments of water molecules within the pore were aligned antiparallel to the helix dipoles. This helped to contribute to the stability of the helix bundle.

Different Alm channel conductance levels correspond to different numbers of helices per bundle, ranging from $N = 5$ to $N > 8$. Calculation of the predicted pK_a values of the ring of Glu18 sidechains at the C-terminal mouth of the pore suggested that at neutral pH most or all of these sidechains will remain protonated. Simulations of $N = 5$, 6, 7 and 8 bundles with a single ionised Glu18 all yielded stable helix bundles. The behaviour of water within these pores was similar to that in the earlier $N = 6$ simulation. Thus, MD simulations in an atomistic bilayer environment support the suggestion that different numbers of Alm helices can self-associate to form a stable helix bundle, at least on the nanosecond timescale.

A similar simulation approach has been applied to the pore domain of the M2 protein from influenza A virus. M2 forms proton permeable channels which are activated at low pH. A combination of mutation studies [136], protein chemistry [137] and spectroscopy [138,139] has been used to demonstrate that the TM segment is α-helical, to identify those residues of the TM helix which seem to line the pore, and to show that the protein tetramerises such that the four TM segments form a parallel helix bundle. Based on this data, two independent modelling studies [137,140] have yielded similar structures [141] for the TM four helix bundle, namely a left-handed supercoil. This has also been seen in simulation studies of the M2 four helix bundle in an octane slab [105]. A number of models of the M2 four TM helix bundle have been simulated in POPC bilayers for periods of up to 4 ns. The details of the simulations differ [142,143], depending on the exact length of M2 which is assumed to be α-helical (see above) and the protonation state of the acidic sidechains at the N-terminal mouth of the pore, but in all cases the a continuous pore is *not* found running through the centre of the bundle. Instead, in all models there is an interior cavity containing just three water molecules, which do not exchange with the exterior. This would suggest that the model corresponds to the closed state of the channel. As it has been suggested [144,145] that protonation of His37 is required to open (activate) the channel, further simulations are needed to explore the open state.

A recent study [146] has illustrated how MD simulations in a bilayer environment may be used as a component of a more general strategy for modelling membrane proteins. Aquaporin (Aqp) is a membrane protein which enables passive transport of water across cell membranes [147]. Prediction studies backed up by experimental topology and spectroscopic data [148] suggest that the Aqp molecule is made up of a single polypeptide chain containing six TM helices. This topology is supported by medium (6–7 Å) resolution EM images of two dimensional crystals of Aqp [149,150] which reveal six rods of density forming a distorted right-handed supercoil. The packing of six TM helices in Aqp was modelled by in vacuo MD simulations in which the helices were restrained [151] to match their proposed positions in the EM images. The resultant model was then 'refined' by embedding it in a phospholipid (POPC) bilayer, solvating the protein/bilayer and running a 1.3-ns MD simulation, *without any restraints* [146]. The 'stability' of the model was measured via the Cα atom RMSD between the initial ($t = 0$) structure and to the structure at the end of the simulation. For Model7 of Aqp1 this was approx. 1.8 Å. Fluctuations in the structure over the course of the simulation were greater for the inter-helix loops than for the TM helices. This suggests that the packing of helices within this model is stable. Of course, the low Cα RMSD does not prove that the model structure is correct. Rather, a low RMSD in such a simulation is a necessary but not a sufficient condition for a correct model. However, the results from this

simulation do suggest that bilayer MD simulations may be used to test and refine models for integral membrane proteins, and in this way may be helpful in the refinement of homology models based on X-ray or EM structures.

7.6. Full bilayer simulations: conclusions

It is tempting to attempt to generalise about the results from explicit bilayer simulations of helix/bilayer interactions. However, we should remember that any such generalisations are being made upon the basis of a small number of simulations, which in themselves are of relatively simple systems. It is quite likely that before reliable general results emerge from such simulations they will have to be extended to both more TM helix species, and to a wider range of bilayer lipids. In particular, it will be of interest to use a systematic series of bilayer simulations to explore the concept of peptide/bilayer mismatch [152] at the atomic level.

A first step towards a more general analysis of peptide/bilayer interactions in simulations has been made by Tieleman et al. [103], who examined lipid/protein interactions in simulations of isolated TM helices (flu M2 and Alm), of helix bundles (again, flu M2 and Alm) and of the porin OmpF. The total simulation time for all these systems amounted to over 24 ns. It was found that whereas single TM helices had only small effects on adjacent lipids, both the helix bundles and OmpF caused a significant perturbation in the ordering of nearby lipid chains. Clearly there is scope for further detailed and systematic studies in this area.

Perhaps one thing which emerges quite clearly from the full bilayer simulation studies is that they are, as yet, unable to address long timescale dynamic changes such as voltage-driven insertion of α-helices into bilayers, or peptide-mediated changes in bilayer structure (such as those which are believed to underlie peptide-induced fusion of bilayers) [28]. Almost certainly simulation of such processes will require application of mean-field methods. However, full bilayer simulations do provide an atomic resolution window into peptide/bilayer interactions on a nanosecond timescale. One challenge for future simulation studies will be to exploit the results of atomistic peptide/bilayer simulations in order to develop better mean field potentials for simulation of mesoscopic events.

8. Conclusions

From the studies discussed in this review it is evident is that simulations can now provide information of helix/bilayer/water interactions at atomic resolutions. However, such simulations are still only feasible for relatively short timescales (up to approx. 10 ns) and for relatively small systems (up to approx. 250 lipid molecules). This precludes their direct use in simulations of events which occur on more extended spatial and temporal scales, e.g. membrane fusion or folding of a protein within a membrane. In contrast, mean field simulations are potentially capable of dealing with such larger scale dynamic events, but at present the mean filed potentials used remain rather approximate. Thus, a major challenge for future simulation studies of helix/bilayer interactions is to exploit the results of atomistic simulations to improve the quality of mean field simulations. This will, in turn, enable the latter to be confidently applied to a wide range of dynamic phenomena in membranes.

9. Glossary

Alm	Alamethicin.
BR	Bacteriorhodopsin.
CD	Circular dichroism.
CFP	Channel forming peptide.
DMPC	1,2-Dimyristoyl-*sn*-glycero-3-phosphatidylcholine.
DPPC	1,2-Dipalmitoyl-*sn*-glycero-3-phosphatidylcholine.
IMP	Integral membrane protein.
MC	Monte Carlo.
MD	Molecular dynamics.
PBC	Periodic boundary conditions.
POPC	1-Palmitoyl-2-oleoyl-*sn*-glycero-3-phosphatidylcholine.
RMSD	Root mean squared deviation.
TM	Transmembrane.

Acknowledgements

Research in MSPS's laboratory is supported by The Wellcome Trust and by the UK–Israel Science and Technology Research Fund. PCB is a Wellcome Trust International Prize Travelling Fellow. Our thanks to Indira Shrivastava for her helpful comments on this manuscript.

References

[1] E. Wallin, G. von Heijne, Protein Sci. 7 (1998) 1029–1038.
[2] K.M. Merz, B. Roux, Biological Membranes: A Molecular Perspective from Computation and Experiment, Birkhäuser, Boston, 1996.
[3] K.M. Merz, Curr. Opin. Struct. Biol. 7 (1997) 511–517.
[4] E. Jakobsson, Trends Biochem. Sci. 22 (1997) 339–344.
[5] D.J. Tobias, K.C. Tu, M.L. Klein, Curr. Opin. Colloid Interface Sci. 2 (1997) 15–26.
[6] D.P. Tieleman, S.J. Marrink, H.J.C. Berendsen, Biochim. Biophys. Acta 1331 (1997) 235–270.
[7] M.S.P. Sansom, Curr. Opin. Struct. Biol. 8 (1998) 237–244.
[8] B. Roux, M. Karplus, Annu. Rev. Biophys. Biomol. Struct. 23 (1994) 731–761.
[9] N. Ben-Tal, A. Benshaul, A. Nicholls, B. Honig, Biophys. J. 70 (1996) 1803–1812.
[10] J.L. Popot, D.M. Engelman, Biochemistry 29 (1990) 4031–4037.
[11] K.V. Pervushin, A.S. Arseniev, FEBS Lett. 308 (1992) 190–196.
[12] A.L. Lomize, K.V. Pervushkin, A.S. Arseniev, J. Biomol. NMR 2 (1992) 361–372.
[13] I.L. Barsukov, D.E. Nolde, A.L. Lomize, A.S. Arseniev, Eur. J. Biochem. 206 (1992) 665–672.
[14] K.S. Huang, H. Bayley, M.J. Liao, E. London, H.G. Khorana, J. Biol. Chem. 256 (1981) 3802–3809.
[15] M.J. Liao, K.S. Huang, H.G. Khorana, J. Biol. Chem. 259 (1984) 4200–4204.
[16] H. Sigrist, R.H. Wenger, E. Kislig, M. Wüthrich, Eur. J. Biochem. 177 (1988) 125–133.
[17] T.W. Kahn, D.M. Engelman, Biochemistry 31 (1992) 6144–6151.
[18] D. Picot, P.J. Loll, M. Garavito, Nature 367 (1994) 243–249.
[19] K.U. Wendt, K. Poralla, G.E. Schulz, Science 277 (1997) 1811–1815.
[20] K.J. Shon, Y.G. Kim, L.A. Colnago, S.J. Opella, Science 252 (1991) 1303–1304.
[21] J.A. Hoffman, Immunol. Today 13 (1992) 411–415.
[22] D. Hultmark, Trends Genet. 9 (1993) 178–183.
[23] M. Zasloff, Curr. Opin. Immunol. 4 (1992) 3–7.
[24] J.A. Hoffman, J.-M. Reichhart, C. Hetry, Curr. Opin. Immunol. 8 (1996) 8–13.
[25] B.L. Kagan, T. Ganz, R.I. Lehrer, Toxicology 87 (1994) 131–149.
[26] B. Bechinger, J. Membr. Biol. 156 (1997) 197–211.
[27] E. Gazit, I.R. Miller, P.C. Biggin, M.S.P. Sansom, Y. Shai, J. Mol. Biol. 258 (1996) 860–870.
[28] M.S.P. Sansom, Curr. Opin. Colloid Interface Sci. 3 (1998) 518–524.
[29] Y. Pouny, D. Rapaport, A. Mor, P. Nicolas, Y. Shai, Biochemistry 31 (1992) 12416–12423.
[30] B. Bechinger, M. Zasloff, S.J. Opella, Protein Sci. 2 (1993) 2077–2084.
[31] K. Matsuzaki, O. Murase, H. Tokuda, S. Funakoshi, N. Fujii, K. Miyajima, Biochemistry 33 (1994) 3342–3349.
[32] S.J. Ludtke, K. He, Y. Wu, H.W. Huang, Biochim. Biophys. Acta 1190 (1994) 181–184.
[33] S.J. Ludtke, W.T. Heller, T.A. Harroun, L. Yang, H.W. Huang, Biochemistry 35 (1996) 13723–13728.
[34] M.S.P. Sansom, Prog. Biophys. Mol. Biol. 55 (1991) 139–236.
[35] M.S.P. Sansom, Q. Rev. Biophys. 26 (1993) 365–421.
[36] G. Baumann, P. Mueller, J. Supramol. Struct. 2 (1974) 538–557.
[37] K. He, S.J. Ludtke, W.T. Heller, H.W. Huang, Biophys. J. 71 (1996) 2669–2679.
[38] B.H. Knowles, D.J. Ellar, Biochim. Biophys. Acta 924 (1987) 509–518.
[39] H. Höfte, H.R. Whitely, Microbiol. Rev. 53 (1989) 242–255.
[40] J. Li, Curr. Opin. Struct. Biol. 2 (1992) 545–556.
[41] W.A. Cramer, J.B. Heymann, S.L. Schendel, B.N. Deriy, F.S. Cohen, P.A. Elkins, C.V. Stauffacher, Annu. Rev. Biophys. Biomol. Struct. 24 (1995) 611–641.
[42] P. Elkins, A. Bunker, W.A. Cramer, C.V. Stauffacher, Structure 5 (1997) 443–458.
[43] M.W. Parker, F. Pattus, Trends Biochem. Sci. 18 (1993) 391–395.
[44] V.E. Bychkova, R.H. Pain, O.B. Ptitsyn, FEBS Lett. 238 (1988) 231–234.
[45] L. Salwinski, C. Levinthal, F. Levinthal, W.L. Hubbel, Biophys. J. 64 (1993) A183.
[46] E. PebayPeyroula, G. Rummel, J.P. Rosenbusch, E.M. Landau, Science 277 (1997) 1676–1681.
[47] S. Iwata, C. Ostermeier, B. Ludwig, H. Michel, Nature 376 (1995) 660–669.
[48] D.A. Doyle, J.M. Cabral, R.A. Pfuetzner, A. Kuo, J.M. Gulbis, S.L. Cohen, B.T. Cahit, R. MacKinnon, Science 280 (1998) 69–77.
[49] J.U. Bowie, J. Mol. Biol. 272 (1997) 780–789.
[50] G.A. Woolley, B.A. Wallace, J. Membr. Biol. 129 (1992) 109–136.
[51] D.S. Cafiso, Annu. Rev. Biophys. Biomol. Struct. 23 (1994) 141–165.
[52] N. Unwin, Nature 373 (1995) 37–43.
[53] M.S.P. Sansom, C. Adcock, G.R. Smith, J. Struct. Biol. 121 (1998) 246–262.
[54] M. Wiener, D. Freymann, P. Ghosh, R.M. Stroud, Nature 385 (1997) 461–464.

[55] D.M. Engelman, T.A. Steitz, Cell 23 (1981) 411–422.
[56] W.G.J. Hol, P.T. van Duijnen, H.J.C. Berendsen, Nature 273 (1978) 443–446.
[57] W.G.L. Hol, Adv. Biophys. 19 (1985) 133–165.
[58] Q.X. Qiu, K.S. Jakes, P.K. Kienker, A. Finkelstein, S.L. Slatin, J. Gen. Physiol. 107 (1996) 313–328.
[59] H. Vogel, Biochemistry 26 (1987) 4562–4572.
[60] C.M. Deber, S.-C. Li, Biopolymers 37 (1995) 295–318.
[61] P. Biggin, J. Breed, H.S. Son, M.S.P. Sansom, Biophys. J. 72 (1997) 627–636.
[62] N. Gibbs, R.B. Sessions, P.B. Williams, C.E. Dempsey, Biophys. J. 72 (1997) 2490–2495.
[63] O. Edholm, F. Jähnig, Biophys. Chem. 30 (1988) 279–292.
[64] F. Jähnig, O. Edholm, J. Mol. Biol. 226 (1992) 837–850.
[65] M. Milik, J. Skolnick, Proteins: Struct. Func. Genet. 15 (1993) 10–25.
[66] M. Milik, J. Skolnick, Biophys. J. 69 (1995) 1382–1386.
[67] P.C. Biggin, M.S.P. Sansom, Biophys. Chem. 60 (1996) 99–110.
[68] P. La Rocca, M.S.P. Sansom, Y. Shai, A. Mor, Protein Sci. 6 (1997) 54.
[69] P. La Rocca, Y. Shai, M.S.P. Sansom, Biophys. Chem. (1999) in press.
[70] H. Heller, M. Shaefer, K. Schulten, J. Phys. Chem. 97 (1993) 8343–8360.
[71] E. Gazit, P. La Rocca, M. Sansom, Y. Shai, Proc. Natl. Acad. Sci. U.S.A. 95 (1998) 12289–12294.
[72] D.T. Edmonds, Eur. Biophys. J. 13 (1985) 31–35.
[73] B. Roux, Biophys. J. 73 (1997) 2980–2989.
[74] P.C. Biggin, D. Phil. Thesis, University of Oxford, 1997.
[75] N. Yang, R. Horn, Neuron 15 (1995) 213–218.
[76] H.P. Larsson, O.S. Baker, D.S. Dhillon, E.Y. Isacoff, Neuron 16 (1996) 387–397.
[77] A. Baumgärtner, Biophys. J. 71 (1996) 1248–1255.
[78] J.L. Cornette, K.B. Cease, H. Margalit, J.L. Spouge, J.A. Berzovsky, C. DeLisi, J. Mol. Biol. 195 (1987) 659–685.
[79] P.A. Karplus, Protein Sci. 7 (1997) 1302–1307.
[80] J.F. Hunt, P. Rath, K.J. Rothschild, D.M. Engelman, Biochemistry 36 (1997) 15177–15192.
[81] C.W. Wimley, S.H. White, Nature Struct. Biol. 3 (1996) 842–848.
[82] H. Kovacs, A.E. Mark, J. Johansson, W.F. van Gunsteren, J. Mol. Biol. 247 (1995) 808–822.
[83] J.S. Richardson, D.C. Richardson, in: G.D. Fasman (Ed.), Prediction of Protein Structure and the Principles of Protein Conformation, Plenum, New York, 1989, pp. 1–98.
[84] S.C. Li, C.M. Deber, FEBS Lett. 311 (1992) 217–220.
[85] C.M. Deber, N.K. Goto, Nature Struct. Biol. 3 (1996) 815–818.
[86] R.B. Sessions, N. Gibbs, C.E. Dempsey, Biophys. J. 74 (1998) 138–152.
[87] K.V. Damodaran, K.M. Merz, B.P. Gaber, Biophys. J. 69 (1995) 1299–1308.
[88] O. Edholm, J. Johansson, Eur. Biophys. J. 14 (1987) 203–209.
[89] C. Chipot, A. Pohorille, J. Mol. Struct. (Theochem.) 398/399 (1997) 529–535.
[90] J.D. Lear, Z.R. Wasserman, W.F. DeGrado, Science 240 (1988) 1177–1181.
[91] K.S. Åkerfeldt, J.D. Lear, Z.R. Wasserman, L.A. Chung, W.F. DeGrado, Acc. Chem. Res. 26 (1993) 191–197.
[92] Q. Zhong, Q. Jiang, P.B. Moore, D.M. Newns, M.L. Klein, Biophys. J. 74 (1998) 3–10.
[93] I.D. Kerr, R. Sankararamakrishnan, O.S. Smart, M.S.P. Sansom, Biophys. J. 67 (1994) 1501–1515.
[94] P. Mitton, M.S.P. Sansom, Eur. Biophys. J. 25 (1996) 139–150.
[95] Q. Zhong, P.B. Moore, D.M. Newns, M.L. Klein, FEBS Lett. 427 (1998) 267–270.
[96] U. Schubert, A.V. Ferrer-Montiel, M. Oblatt-Montal, P. Henklein, K. Strebel, M. Montal, FEBS Lett. 398 (1996) 12–18.
[97] P.B. Moore, Q. Zhong, T. Husslein, M.L. Klein, FEBS Lett. 431 (1998) 143–148.
[98] A. Grice, I.D. Kerr, M.S.P. Sansom, FEBS Lett. 405 (1997) 299–304.
[99] M.S. Weiss, U. Abele, J. Weckesser, W. Welte, E. Schiltz, G.E. Schulz, Science 254 (1991) 1627–1630.
[100] M. Schiffer, C.H. Chang, F.J. Stevens, Protein Eng. 5 (1992) 213–214.
[101] W.M. Yau, P.J. Steinbach, W.C. Wimley, S.H. White, K. Gawrisch, Biophys. J. 74 (1998) A303.
[102] A. Grossfield, T.B. Woolf, Biophys. J. 74 (1998) A303.
[103] D.P. Tieleman, L.R. Forrest, H.J.C. Berendsen, M.S.P. Sansom, Biochemistry 37 (in press, 1999) 17554–17561.
[104] L.R. Forrest, D.P. Tieleman, M.S.P. Sansom, Biophys. J. (in press, 1999).
[105] Q. Zhong, T. Husslein, P.B. Moore, D.M. Newns, P. Pattnaik, M.L. Klein, FEBS Lett. 434 (1998) 265–271.
[106] T.B. Woolf, A. Grossfield, K. MacKenzie, D. Engelman, Biophys. J. 74 (1998) A15.
[107] K.R. MacKenzie, J.H. Prestegard, D.M. Engelman, Science 276 (1997) 131–133.
[108] L. Shen, D. Bassolino, T. Stouch, Biophys. J. 73 (1997) 3–20.
[109] K. Belohorcova, J.H. Davis, T.B. Woolf, B. Roux, Biophys. J. 73 (1997) 3039–3055.
[110] T.B. Woolf, B. Roux, Proteins: Struct. Func. Genet. 24 (1996) 92–114.
[111] T.B. Woolf, Biophys. J. 73 (1997) 2376–2392.
[112] T.M. Gray, B.M. Matthews, J. Mol. Biol. 175 (1984) 75–81.
[113] T.B. Woolf, Biophys. J. 74 (1998) 115–131.
[114] D.M. Engelman, T.A. Steitz, A. Goldman, Annu. Rev. Biophys. Biophys. Chem. 15 (1986) 321–353.
[115] D.P. Tieleman, H.J.C. Berendsen, Biophys. J. 74 (1998) 2786–2801.
[116] D.P. Tieleman, M.S.P. Sansom, H.J.C. Berendsen, Biophys. J. 76 (1999) 40–49.

[117] G. von Heijne, J. Mol. Biol. 225 (1992) 487–494.
[118] D.T. Jones, W.R. Taylor, J.M. Thornton, Biochemistry 33 (1994) 3038–3049.
[119] M. Czerzo, E. Wallin, I. Simon, G. von Heijne, A. Elofsson, Protein Eng. 10 (1997) 673–676.
[120] B. Persson, P. Argos, J. Mol. Biol. 237 (1994) 182–192.
[121] B. Rost, P. Fariselli, R. Casadio, Protein Sci. 5 (1996) 1704–1718.
[122] M.S.P. Sansom, L.R. Forrest, R. Bull, Bioessays 20 (1998) 992–1000.
[123] W. Fischer, L.R. Forrest, G.R. Smith, M.S.P. Sansom, Proc. Natl. Acad. Sci. U.S.A. (submitted, 1999).
[124] I.H. Shrivastava, C. Capener, L.R. Forrest, M.S.P. Sansom, Biophys. J. (submitted, 1999).
[125] I.D. Kerr, H.S. Son, R. Sankararamakrishnan, M.S.P. Sansom, Biopolymers 39 (1996) 503–515.
[126] E. Perozo, D.M. Cortes, L.G. Cuello, Nature Struct. Biol. 5 (1998) 459–469.
[127] F. Zhou, K. Schulten, Proteins: Struct. Func. Genet. 25 (1996) 12–27.
[128] P. Huang, G.H. Loew, J. Biomol. Struct. Dyn. 12 (1995) 937–956.
[129] B. Roux, T.B. Woolf, in: K.M. Merz (Ed.), Biological Membranes: A Molecular Perspective from Computation and Experiment, Birkhäuser, Boston, 1996, 587 pp.
[130] S. Bernèche, M. Nina, B. Roux, Biophys. J. 75 (1998) 1603–1618.
[131] P. La Rocca, M.S.P. Sansom, Biochem. Soc. Trans. 26 (1998) S302.
[132] O. Edholm, O. Berger, F. Jähnig, J. Mol. Biol. 250 (1995) 94–111.
[133] D.P. Tieleman, H.J.C. Berendsen, M.S.P. Sansom, Biophys. J. [in press, 76 (1999)].
[134] D.P. Tieleman, J. Breed, H.J.C. Berendsen, M.S.P. Sansom, Faraday Disc. [in press, 111 (1999)].
[135] J. Breed, R. Sankararamakrishnan, I.D. Kerr, M.S.P. Sansom, Biophys. J. 70 (1996) 1643–1661.
[136] L.J. Holsinger, D. Nichani, L.H. Pinto, R.A. Lamb, J. Virol. 68 (1994) 1551–1563.
[137] L.H. Pinto, G.R. Dieckmann, C.S. Gandhi, C.G. Papworth, J. Braman, M.A. Shaughnessy, J.D. Lear, R.A. Lamb, W.F. DeGrado, Proc. Natl. Acad. Sci. U.S.A. 94 (1997) 11301–11306.
[138] K.C. Duff, S.M. Kelly, N.C. Price, J.P. Bradshaw, FEBS Lett. 311 (1992) 256–258.
[139] F.A. Kovacs, T.A. Cross, Biophys. J. 73 (1997) 2511–2517.
[140] M.S.P. Sansom, I.D. Kerr, G.R. Smith, H.S. Son, Virology 233 (1997) 163–173.
[141] L.R. Forrest, W.F. DeGrado, G.R. Dieckmann, M.S.P. Sansom, Folding Design 3 (1998) 443–448.
[142] L.R. Forrest, M.S.P. Sansom, Biochem. Soc. Trans. 26 (1998) S303.
[143] L.R. Forrest, D.P.T. Tieleman, M.S.P. Sansom, Biophys. J. (in preparation, 1999).
[144] C. Wang, R.A. Lamb, L.H. Pinto, Biophys. J. 69 (1995) 1363–1371.
[145] I.V. Chizhmakov, F.M. Geraghty, D.C. Ogden, A. Hayhurst, M. Antoniou, A.J. Hay, J. Physiol. 494 (1996) 329–336.
[146] M.S.P. Sansom, I.D. Kerr, R. Law, R. Davison, D.P. Tieleman, Biochem. Soc. Trans. 26 (1998).
[147] M.J. Chrispeels, P. Agre, Trends Biochem. Sci. 19 (1994) 421–425.
[148] G.M. Preston, J.S. Jung, W.B. Guggino, P. Agre, J. Biol. Chem. 269 (1994) 1668–1673.
[149] A. Cheng, A.N. van Hoek, M. Yeager, A.S. Verkman, A.K. Mitra, Nature 387 (1997) 627–630.
[150] T. Walz, T. Hirai, K. Murata, J.B. Heymann, B.L. Smith, P. Agre, A. Engel, Nature 387 (1997) 624–627.
[151] M.S.P. Sansom, R. Sankararamakrishnan, I.D. Kerr, Nature Struct. Biol. 2 (1995) 624–631.
[152] O.G. Mouritsen, M. Bloom, Annu. Rev. Biophys. Biomol. Struct. 22 (1993) 145–171.